
Satellites Turn “Concrete”: Tracking Cement with Satellite Data and Neural Networks

Alexandre d’Aspremont,¹ Simon Ben Arous,² Jean-Charles Bricongne,³ Benjamin Lietti,⁴ Baptiste Meunier⁵

June 2023, WP #916

ABSTRACT

The Covid crisis has demonstrated the need for alternative data, in real-time and with global coverage. This paper exploits daily infrared images from satellites to track economic activity in advanced and emerging countries. We first develop a framework to read, clean and exploit satellite images. We construct an algorithm based on the laws of physics and machine learning to detect the heat produced by cement plants in activity. This allows to monitor in real-time if a cement plant is functioning. Using this information on more than 500 plants, we construct a satellite-based index tracking activity. Using this satellite index outperforms benchmark models and alternative indicators for nowcasting the activity in the cement industry and in the construction sector. Exploring the granularity of daily and plant-level data, using neural networks yields significantly more accurate predictions. Overall, combining satellite images and machine learning allows to track industrial activity accurately.

Keywords: Data Science, Big Data, Satellite Data, Machine Learning, Nowcasting, Cement, Construction, Industry, Economic Activity, Neural Network.

JEL classification: C51, C81, E23, E37

- (1) CNRS, ENS, Kayrros SAS.
- (2) Kayrros SAS.
- (3) Banque de France, Laboratoire d’Economie d’Orléans, LIEPP/Sciences Po Paris and Paris I University.
- (4) Université Paris-Saclay. benjamin.lietti@gmail.com
- (5) European Central Bank, Aix-Marseille School of Economics (AMSE). baptiste.meunier@ecb.europa.eu

We are very grateful to N. Woloszko, G. Verdugo, S. Laurent, J. Marcucci, P. Altmeyer, M. Esguerra, J. Kaub, participants of the BCEAO workshop on forecasting during crisis (Sept. 21), the FRB – Bank of Canada conference on non-traditional data (Nov. 21), IBFI seminar on big data (Mar. 22), seminar at French *Direction Générale des Entreprises* (Oct. 22), Banque de France internal seminar (Jan. 23), PSE research seminar (Mar. 2023), and AFSE (June 23) for useful comments. This work was supported by the French National Research Agency Grant ANR-17-EURE-0020, and by the Excellence Initiative of Aix-Marseille University - A*MIDEX.

Working Papers reflect the opinions of the authors and do not necessarily express the views of the Banque de France or other institutions of affiliation. This document is available on publications.banque-france.fr/en

NON-TECHNICAL SUMMARY

The assessment of economic activity from space would be of great interest as satellite data are released in near-real-time, have a global coverage with uniform quality, and are free-to-use. Combining these advantages contrasts with usual data sources most often released with a significant lag, whose quality and reliability change much across countries, and which be costly. In addition, the increasing number of satellites, their sophistication and the release of their data in the public domain has made satellite data an increasingly promising source of real-time information.

However, tracking the economy with satellites requires a signal that can be seen from outer space: to that end, we exploit the heat produced by cement plants. Manufacturing cement indeed includes a step where raw materials are heated at about 1,450°C in large ovens called rotary kilns. Such heat can be detected, when using satellite images in the infrared spectrum. There are other interests of focusing on the cement industry since: (i) cement is a widely used commodity, necessary in both advanced and developing economies, and (ii) cement is generally consumed locally, as its low cost makes it unprofitable to ship across long distances. Using these satellite images is a first contribution of this paper, while the literature trying to exploit satellite data has so far focused on night lights (Donaldson and Storeygard, 2016) and more recently on air pollution (Bricongne et al., 2021).

We lay out a method to exploit infrared satellite images and detect automatically heat, using the law of physics and machine learning. The idea of heat detection comes from Planck's law which describes the reflectance (electromagnetic radiation) emitted by an object. By looking at infrared satellite images over the locations of the rotary kilns (ovens) of cement plants, we apply a suite of algorithms based on Planck's law to see whether the kiln is working or not. The left-hand side of Figure N1 shows an example of a working cement plant with different "hot" kilns (in red). The same cement plant is shown during the Covid-19 lockdown in the right-hand side of Figure N1, where no heat is detected as the plant had been completely shut down. We apply this procedure on around 500 cement plants globally to assess their activity. The satellite data are also corrected for cloudiness – using an AI algorithm for image recognition – and interpolated – using extreme gradient boosting, a machine learning algorithm. In the end, this provides a real-time satellite-based index of activity in cement plants, daily and for each plant we track. A second contribution is to set such a procedure to read, exploit, and clean satellite images, combining algorithms based on physics with machine learning.

We then test the predictive power of our satellite-based activity index to nowcast production of cement and broader activity in the construction sector. We find that it outperforms benchmarks, including models based on alternative indicators. We start with a linear model using the satellite index and an AR term to nowcast the production of cement. We find that it outperforms usual benchmarks (random walk and autoregressive model) as well as similar linear models based on construction indicators (building permits, PMI Indices, and Google Trends). But while this 1st model uses the satellite index aggregated at monthly frequency and at country level, in a 2nd step, we explore the granularity of our daily and plant-level satellite indices. We use a MIDAS to exploit the daily frequency, a LASSO to exploit the plant dimension, and a LASSO-MIDAS to explore both these spatial and temporal dimensions. We find however that the accuracy is on average similar when using such models on disaggregated data – compared to the OLS model using data aggregated at monthly frequency and country-level.

We finally use neural networks to predict the production of cement and find that it can significantly outperform the OLS model. Neural networks are highly flexible non-linear methods which have the double advantage of: (i) high flexibility, and (ii) being found in the recent machine learning literature

to outperform other approaches. In line with literature, we employ a multi-layer perceptron with few hidden layers given the small sample size. Overall, neural networks strongly outperform the linear model, and thus also benchmark models. This is another contribution: neural networks can be relevant for nowcasting in macroeconomics – complementing recent applications to nowcast GDP (Woloszko, 2020) and trade (Hopp, 2021).

Figure N1. Satellite images of a cement plant (LHS: Dec. 2019; RHS: Feb. 2020)

Sources: authors, Kayrros SAS



Note: “Hot” pixels are coloured in red

« Satellites turn concrete » ou comment suivre la production de ciment grâce aux données satellites et aux réseaux de neurones

RÉSUMÉ

La crise de la Covid-19 a démontré la nécessité d'utiliser des données alternatives, disponibles en temps réel, avec une couverture globale. Cet article exploite des images satellites infra-rouge pour suivre l'activité économique dans les pays avancés et émergents. Un cadre pour lire, nettoyer et exploiter les images satellites est d'abord développé. Un algorithme basé sur les lois de la physique et les techniques d'apprentissage automatique est construit pour détecter la chaleur produite par les usines de ciment en activité. Cela permet de détecter en temps réel si une usine de ciment est en train de produire. Utilisant cette information sur plus de 500 usines, nous construisons un indice basé sur les données satellites qui suit l'activité. L'utilisation de cet indice basé sur données satellites affiche de meilleures performances que des modèles de référence et des indicateurs alternatifs pour le nowcasting de la production de l'industrie du ciment ainsi que pour l'activité du secteur de la construction. En exploitant la granularité de nos données journalières et disponibles au niveau des usines, nous trouvons qu'une utilisation des réseaux de neurones permet d'obtenir des prévisions de meilleure qualité. Dans l'ensemble, la combinaison d'images satellites et d'apprentissage automatique permet un suivi adéquat de l'activité industrielle.

Mots-clés : science des données, big data, données satellites, apprentissage automatique, nowcasting, ciment, construction, industrie, activité économique, réseaux de neurones

Les Documents de travail reflètent les idées personnelles de leurs auteurs et n'expriment pas nécessairement la position de la Banque de France ou des autres institutions d'affiliation. Ils sont disponibles sur publications.banque-france.fr

Introduction

While official statistics on construction are in general scarce and face long publication delays, the multiplication of satellites (from 1,033 in 2011 to 4,877 in 2021),¹ the sophistication of their on-board instruments, and the release of their data in the public domain has made satellite data an increasingly relevant source of real-time information. Not only data from satellite constellations like the EU's SENTINEL are free to use, but they also have a global coverage with uniform quality – since gathering information from space does not discriminate between levels of development, aptitudes of statistical agencies, or distortions in reporting. This makes satellite data particularly relevant for cross-country analysis. Another key advantage of satellite data is their timeliness, with data usually released the day following the capture. As such, satellite data appear suitable to fill the need for global, timely, and real-time data.

Against this background, this paper exploits satellite images – a data source mostly untapped in the economic literature – to provide a real-time indicator of economic activity. The idea is to track the production of cement plants given that (i) they emit a sizeable amount of heat which can be seen from satellites, (ii) cement is a widely used commodity, and to a large extent locally produced, and (iii) their production correlates with activity in the construction sector, itself found to be an early indicator of the economic cycle (Bon, 1992; Lean, 2001). We start by identifying the locations for more than 500 cement plants and get satellite infrared images over these locations taken by the ESA's SENTINEL-2 satellites. Then, building on Planck's law that describes the density of infrared bands for "hot" objects, we construct an algorithm to detect whether the kilns (rotary ovens where cement is heated) are active. We correct satellite images for cloudiness – using an AI algorithm for image recognition – and interpolate missing points – using extreme gradient boosting, a machine learning algorithm. In the end, this procedure provides us with a real-time satellite-based index of activity in cement plants, daily and for each of the 500 plants we track.

We then test the predictive power of our satellite-based activity index and find it outperforms benchmarks and alternative indicators, when using a linear framework (OLS) and even more so when relying on neural networks. We start with a linear model to nowcast the production of cement. We find that it outperforms benchmarks (random walk and autoregressive model) as well as similar linear models based on usual early indicators of the construction sector (building permits, Purchasing Managers Index, and Google Trends). While this first model uses the satellite index aggregated at *monthly* frequency and at *country level*, in a second step, we explore the granularity of our *daily* and *plant-level* satellite indices. We use MIDAS, LASSO, and LASSO-MIDAS to explore spatial and/or temporal dimensions: we find that the accuracy is on average similar when using our satellite index aggregated or disaggregated. We finally turn to exploring non-linearities between cement production and our satellite index, using an

¹ Source: Statista; of which 446 are dedicated to Earth observation. The trend is likely to even accelerate, with an average of around 1,000 new satellites expected to be launched each year until 2028 (source: Euroconsult).

ensemble of neural networks. Overall, neural networks are found to strongly outperform the linear model, and thereby also benchmark models as well as models based on usual indicators for construction. We finally move beyond the cement industry and nowcast the activity in the whole construction sector. Results suggest that the satellite-based activity index retains a high informative power for the whole construction sector.

This paper contributes to the literature by laying an innovative methodology to exploit satellite images, a data source largely uncharted in economics so far. Our approach also relies on innovative techniques in economics: the interpolation of data is based on gradient boosting, cloud detection uses AI-based image recognition, and best-performing predictions are based on neural networks. In that sense, this paper contributes to the broad literature on forecasting by making use of various innovative techniques. The paper also contributes to the literature on tracking economic activity by adding a new source of relevant data, showing how to exploit infrared satellite images. This complements efforts already taken in economics to use satellite data, but which have predominantly relied on night-time light intensity in order to predict GDP. We do not only complement this literature with another data source, but also, evidence in this paper suggests that satellite infrared images retain their predictive power for advanced economies and high-density regions – while the literature has shown “night lights” to face difficulties over such areas. Finally, this paper contributes to the literature on high-frequency data. In this growing field, this paper adds an innovative data source with a global coverage, a uniform quality across all countries, a near real-time release, and a high granularity – while alternative high-frequency data often miss some of these qualities. Finally, this paper adds a real-time indicator for monitoring the construction sector while the literature has highlighted the lack of reliable early indicators, even for advanced economies.

The rest of the paper is organised as follows: **section 1** reviews the related literature, **section 2** describes satellite data and provides a method to detect heat on satellite images. **Section 3** details data cleaning based on machine learning. **Section 4** compares the nowcasting performances across different types of models, notably an ensemble of neural networks, and for both cement production and volume of construction. The last section concludes.

Section 1: Literature review

This paper first relates to the literature using satellite data for tracking economic conditions. A large strand of this literature has relied on night-time luminosity. Among this rich literature (see Donaldson and Storeygard, 2016 for a review), most have used it to evaluate income in developing countries (Ebener et al., 2005; Ghosh et al., 2009; Henderson et al., 2012; Pinkovskiy and Sala-i-Martin, 2016). There have also been more specific uses: Civelli et al. (2018) track the impact of foreign aid on growth in Uganda; Chodorow-Reich et al. (2020) measure the impact of India’s demonetization; and Beyer et al. (2021) examine the impact of Covid-19 in India. But

limits have been documented, notably that these data lose their informative power over high-density areas and advanced economies (Sutton et al., 2007; Chen and Nordhaus, 2010). Tanaka and Keola (2017) even report similar difficulties over Cambodia. This has pushed economists to rely on other satellite data, such as Bricongne et al. (2021) using data on NO₂ pollution for nowcasting industrial production.

Compared to this literature, this paper uses an uncharted type of satellite data. Only very few papers have exploited infrared satellite images (e.g. Combinido et al., 2018 for estimating cyclone intensity; Scambos et al., 2018 for assessing surface temperature in Antarctica) and this paper is the first one to do so in economics – to the best of our knowledge. Our paper stands out by (i) proposing an alternative data treatment method based on machine learning, (ii) covering a much larger geographic area, and (iii) applying this index for nowcasting. Compared to the literature on “night lights”, evidence suggests that infrared satellite-image-based activity index of activity still has predictive power for advanced countries.

This paper also relates to the nascent literature on alternative high-frequency data, adding an innovative dataset with global coverage, uniform quality across countries, near real-time release, high granularity, and based on open-source data. In the wake of the Covid-19 crisis, a number of new datasets have emerged such as weekly card spending (Carvalho et al., 2020), daily housing online listings (Bricongne et al., 2023) or hourly electricity consumption (Chen et al., 2020).² This paper adds to this list while also going one step further. First, the data presented here have a global coverage with uniform quality across countries, which is not the case in most alternative datasets – for example Google data which are not available for some countries (for example China where Google is banned) and whose quality depends on Google’s market penetration. The second contribution is that besides delivering an innovative indicator, this paper explores to what extent such data enhance real-time forecasting.

By building a real-time and tailored-made index for activity in the cement industry, this paper overcomes the lack of valid and transparent data on construction, an issue raised by Ruddock and Lopes (2006), Hahn and Skudelny (2008), as well as Gomez and del Carmen Sanchez (2017), and even more pregnant for high-frequency indicators (Aaronson et al., 2016). In general, the literature on forecasting construction has focused on the demand side (Uzzaman et al., 2016). On the contrary, this paper provides a real-time picture of the supply side, assessing the level of activity in the manufacture of cement. While most of the literature has relied on time series methods such as ARIMA (Wilinski et al., 2016) and on weather factors (Kalvova et al., 2003). In addition, papers generally link the activity in construction to long-term trends such as demographics or development (Li et al., 2016; Deakshinamurthy, 2017) and therefore do not cover short-term variations.

² For reviews of some innovative datasets that have been put into use during the Covid-19 crisis, see Chetty et al. (2020) for the US and Bricongne et al. (2020) for France.

Finally, this paper contributes to the literature on forecasting, not only by using innovative satellite images, but also by relying on neural networks – a machine learning technique with only limited use so far in economics. Examples include Woloszko (2020) building GDP tracker based on neural networks and Google Trends, as well as Hopp (2021) for forecasting trade. Joseph (2019) had nonetheless demonstrated the potential of this method for economic analysis, while also noting that some economists can be sceptical about the “black box” nature of neural networks.³ Buckmann and Joseph (2022) have also laid out a framework for economic forecasting with machine learning, with a focus on interpretability. This paper adds another example of forecasting with neural network, showing sizeable improvements over a linear model.

Section 2: Data

1. *Why focusing on cement?*

Cement is widely used in all economies across the globe, regardless of their state of development. On top of the construction of new infrastructure such as roads, factories, residential units, dams, or ports, cement also plays a predominant role in the maintenance of these infrastructures (Gagg, 2014). As a result, cement is the second most consumed commodity in the world – after only water. Focusing on construction, the quantity of cement used is twice as much as the sum of all other materials combined.⁴

In turn, the construction sector has been identified as an early indicator of the business cycle in the literature. The relationship between construction and economic development had long been documented (Strassmann, 1970) notably for advanced economies (Bon and Pietroforte, 1990; de Long and Summers, 1991). Recent studies showed a similar pattern for developing economies and evaluated causality. Hong (2014) shows that real-estate investments are positively correlated to economic growth in China in the short run. This has been corroborated for Turkey by Berk and Bicen (2018) and for African countries in Alagidede and Mensah (2018). Kumo (2012) goes beyond and shows that infrastructure investment Granger-causes activity in the private sector for South Africa. In the meantime, papers such as Jiang (2013) suggest that the relationship between construction and GDP remains valid in advanced economies even though the share of construction in GDP has declined. These papers also find the relationship to be significant in the short run, suggesting that activity in the construction sector could be an adequate proxy for economic activity.

Third, cement is generally produced and consumed locally – therefore providing information on local economic activity. The relatively low price of cement for a given volume makes it

³ The interpretability aspect is less pregnant in this paper where the objective is less to explain which variables are most informative than to reach maximum accuracy.

⁴ Source: European Cement Association (CEMBUREAU).

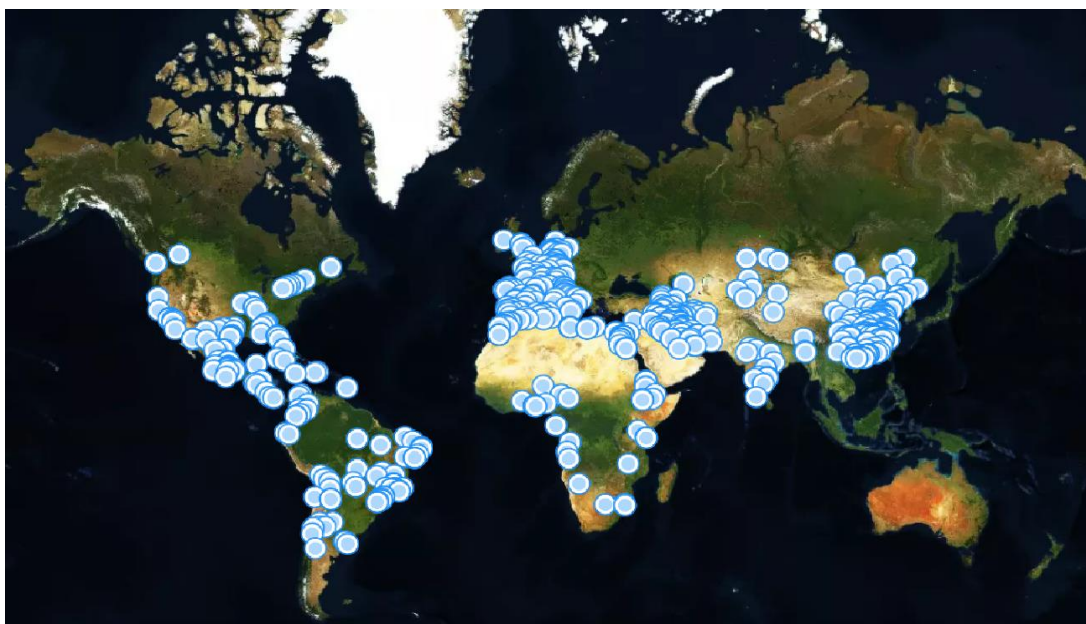
unprofitable to trade over long distances, in particular through road transportation.⁵ Even though some cross-countries trade occurs, mostly by shipping, the quantities remain limited so that local production highly correlates with local use.⁶ Empirically, this is confirmed in our dataset with an average correlation of 0.71 between the volume of construction and the volume of production in the cement industry.

2. *How to capture cement production with satellites?*

Interestingly, the production of cement generates a sizable amount of heat which can be detected on satellite infrared images. To produce cement, a key step after the extraction of raw materials (limestone, shale, clay, iron ore, silica sand, others) is the heating of a mix of those raw materials in rotary kilns (type of thermally insulated chamber, or in non-technical terms, an oven) at a temperature of about 1,450°C. This triggers a chemical reaction ending in the synthesis of clinker, an intermediary product in the manufacture of cement. This step can be detected on satellite images given the high temperature needed. The clinker is then cooled and grounded down with some additives (mainly gypsum and anhydrite) to form the finished product: ready-to-use cement.

Figure 1. Localisation of cement plants under monitoring

Sources: authors, Kayrros SAS



This requires having the location of each cement plant in order to retrieve satellite images over these specific areas. Based on industry information, we obtain coordinates for a large set of 521 cement plants across 42 advanced and developing countries, as shown in **Figure 1**.⁷ As

⁵ According to CEMBUREAU, shipping cement across the Atlantic is cheaper than transporting it by truck over 300 km.

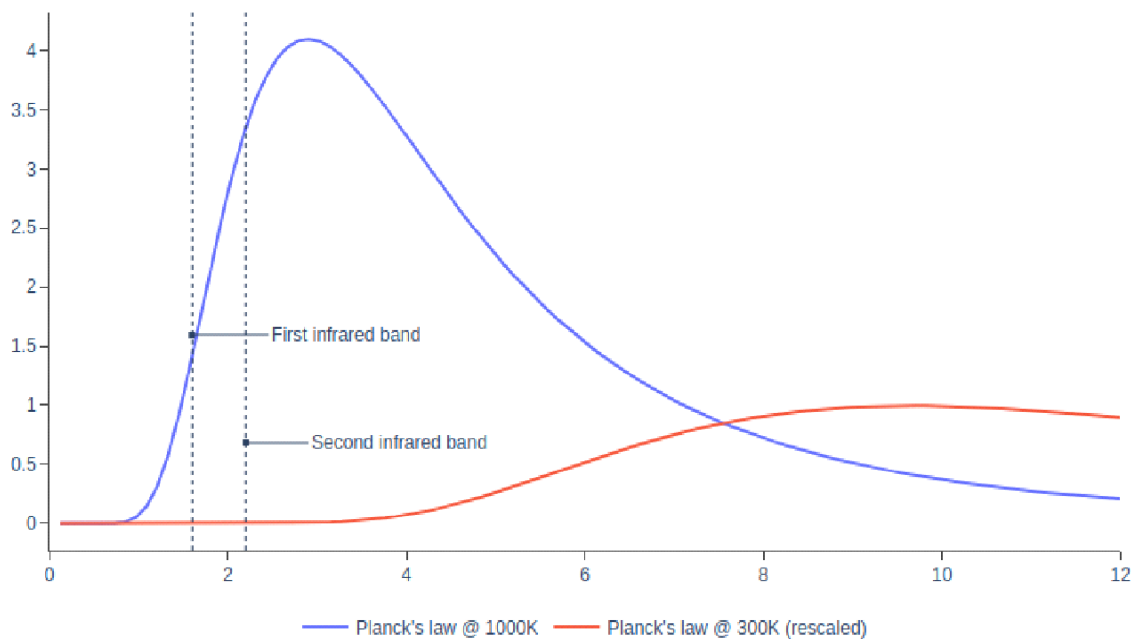
⁶ For example, for France, less than 10% of the total cement production is exported. Source: INSEE.

⁷ The list of cement plants is as of July 2021; it is continuously extended by Kayrros SAS to reach full coverage.

one cement plant can have more than one kiln, this amounts to more than 700 kilns. Once all the coordinates are obtained, the first step for our method consists in obtaining the satellite infrared images for all cement plants at different points in time.

Once satellite images are recovered over each cement plant, we set up a robust method to automatically identify the heat emitted by the kilns. We do so by using modern satellite equipped with near-infrared and short-wave infrared sensors able to capture a large spectrum of wavelengths. More specifically, we rely on satellites SENTINEL-2A and 2B, placed into orbit by the European Space Agency (ESA) respectively in 2015 and 2017, and equipped with such modern optical instruments. The resolution of images collected by these satellites covers a surface of 20 square metres (at ground level) per pixel with a mean revisit time of 3.8 days.

Figure 2. Planck’s law and wavelengths distribution at different temperatures
(band on x-axis, reflectance in y-axis)
Sources: authors, Kayrros SAS



We detect if a kiln is “hot” – indicating that clinker is being produced – by applying the heat-detection algorithm HOTMAP based on Planck’s law. In a nutshell, Planck’s law characterises the distribution of wavelengths emitted by an object at different temperatures. The contrast between two bands can be large at high temperatures. **Figure 2** shows for example that the reflectance (y-axis) for the first two infrared bands (x-axis) is similar at 300°K (red line) but significantly different at 1000°K (blue line). The HOTMAP method, developed by Murphy et al. (2016) and expanded by Massimetti et al. (2020), exploits this principle and flags “hot” pixels on an image based on the contrasts in reflectance between the infrared bands 8a, 11, and 12. The broad idea is that infrared bands with longer wavelengths are more sensitive to heat than those with shorter wavelengths. More specifically, a pixel is flagged “hot” if it meets one of the three conditions below where ρ_i is the reflectance of band i .

$$(1) \quad \frac{\rho_{12}}{\rho_{11}} \geq 1.4 \text{ and } \frac{\rho_{12}}{\rho_{8a}} \geq 1.2 \text{ and } \rho_{12} \geq 0.15$$

$$(2) \quad \frac{\rho_{11}}{\rho_{8a}} \geq 2 \text{ and } \rho_{11} \geq 0.5 \text{ and } \rho_{12} \geq 0.5$$

$$(3) \quad [\rho_{12} \geq 1.2 \text{ and } \rho_{8a} \leq 1] \text{ or } [\rho_{11} \geq 1.5 \text{ and } \rho_{8a} \geq 1]$$

Condition (1) flags “hot” pixels as band 12 is expected to be more sensitive to heat than bands 8a and 11; the rightmost inequality ($\rho_{12} \geq 0.15$) ensures that the reflectance of band 12 is large enough to avoid false positives – which can happen over low-reflectance areas such as water. Condition (2) flags “very hot” pixels with band 11 at least twice more reflective than band 8a, and high reflectance for both bands 11 and 12. Condition (3) detects saturation of bands 11 and 12 that happen over “extremely hot” pixels, with the thresholds calibrated empirically by Massimetti et al. (2020) on a volcanic eruption.

To minimize the number of false positives in heat detection, the classification of “hot” pixels by the HOTMAP method is complemented by a second algorithm (ASE). In a first step, the HOTMAP method above flags “hot” pixels. But as it can identify false positives, flagged pixels are further checked through the Autonomous Sciencecraft Experiment (ASE) method (see for example Chien et al., 2005). In this approach, pixels are deemed “hot” if the spectral gradient g between bands 11 and 12, defined as $g = \frac{(\rho_{12} - \rho_{11})}{(\rho_{12} + \rho_{11})}$, exceeds a threshold. This method is again based on Planck’s law and the fact that infrared bands with longer wavelengths are more sensitive to heat. In our method, the ASE is used to cross-check the pixels that have been first flagged “hot” by the HOTMAP method. Only those pixels whose gradient g is greater than a country-specific threshold are kept considered “hot”. For both heat-detection algorithms (HOTMAP and ASE), we set country-specific thresholds to account for country specificities notably in the meteorological conditions which greatly influence the reflectance of the bands.⁸ This follows the recent literature on remote sensing showing that temperature induces spectral features modifications such as peak position shifts, band area and peak intensity changes in the infrared spectrum (Munro et al., 2019; Poggiali et al., 2021).

⁸ For the HOTMAP algorithm, we perform a grid search with small variations around the values provided in the literature. For the ASE algorithm, the grid search is between 0.01 and 0.06 as no reference point has been provided in the literature. Bounds of 0.01 and 0.06 are based on empirical observations of the heat produced by kilns. The optimization is conducted with the Python library “Optuna” (Akiba et al., 2019) and is based on a 4-fold cross-validation, using 2018-2019 as train sample and 2020 as test sample. The rest of the sample is kept out of cross-validation to avoid overfitting and is used as a validation set: results point to no overfitting as performances remain robust on this sample. Empirically, setting a country-specific threshold significantly improves accuracy. For example, using thresholds calibrated for China to compute the satellite-based activity index in the US provides a 66% correlation between this index and ground observations. Setting a US-specific threshold raises correlation to 87%. On top of the country-specific calibration of thresholds, a season-specific calibration was tested where thresholds can be differed each month. While results were adequate – in terms of the correlation between satellite-based activity index and ground observations, one main setback was a risk of overfitting as cement production data is itself seasonal. We therefore applied only the country-specific calibration.

The combination of HOTMAP and ASE method produces an index more strongly correlated with ground observations for cement production than individual methods alone. For instance, experiments on Chinese data based solely on the ASE method gave a correlation around 60% between ground and satellite observations. By comparison, combining HOTMAP and ASE raises the correlation to around 90%. **Figure 3** shows examples of satellite images for a cement plant in China: the left-hand side is at end 2019 with rotary kilns hot (red); the right-hand side shows the same plant at the height of the Covid-19 pandemic with no heat detected.

Figure 3. Satellite images of a cement plant in China (LHS: Dec. 2019, RHS: Feb. 2020)

Sources: authors, Kayrros SAS



Note: Pixels flagged “hot” by the sequence of algorithms are coloured in red

Applying this process to satellite images at different points in time for each cement plant provides a satellite-based time series of plant activity. Once we identify “hot” pixels on satellite image, we build a binary activity index for each kiln of the cement plant, assigning value 1 if the kiln is in activity (“hot”) and 0 otherwise. Once such a binary index is obtained for each kiln in the cement plant, we aggregate at plant level. For a plant with n kilns ($n > 1$), this aggregated index is $\frac{n_{hot}}{n}$, or in other words the ratio of hot kilns (n_{hot}) over the total number of kilns (n).⁹

3. Data sources for cement production and volume of construction

Cement production is obtained from national statistical agencies. **Table A1.1** in **Annex 1** details data sources. When data for the production of cement are not available, we instead take the volume of production for the parent aggregate. For instance, in NACE2 classification, when volumes for the production of cement (C23.51) were not available, we take data for the production of cement, lime and plaster (C23.5); then if also not available, we look at production of other non-metallic mineral products (C23). And in the rare cases where none of the latter is available, we consider the volume of production in the whole manufacturing sector (C).

⁹ While this implicitly assumes that a plant capacity is proportional to its number of active kilns, this is based on industry insights that kilns have generally a similar capacity due to standards of production.

As regards activity in the construction sector, data are taken from national or international statistical agencies. For European countries, data also come from Eurostat. For the US, volume of construction is taken from the US Census Bureau. For other countries, data are taken from the OECD database on the monthly Main Economic Indicators (MEI) for construction.

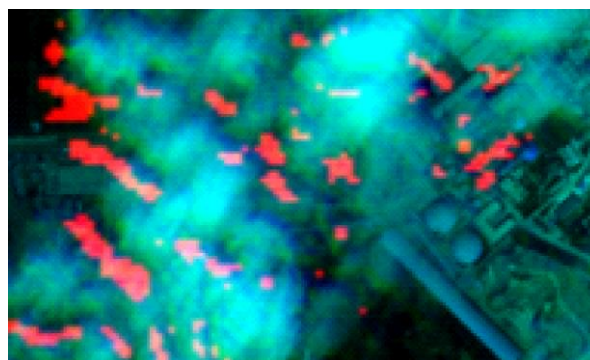
Section 3: Data cleaning

1. Filtering clouds

Since the infrared-based detection of heat can be biased by clouds, we identify the cloudiness for each satellite image using an AI-based image recognition method. On infrared images, clouds affect the reflectance of the infrared bands used for heat detection, due to the humidity brought by clouds. As shown in **Figure 4** – on which “hot” pixels are coloured in red – clouds distort the results of the HOTMAP-ASE algorithm and lead to the erroneous detection of “hot” pixels. Cloud masks are detected using an AI-based algorithm of image recognition on the RGB image, which automatically flag the presence of clouds based on the shift in phase between colour bands, producing an output similar to **Figure 5** (right-hand side). We then compute an index of cloudiness taking values between 0 and 1 which is the proportion of the image affected by the cloud mask. Based on this index, we filter out observations with high cloud coverage.¹⁰

Figure 4. Effects of clouds on heat detection (“hot” pixels in red)

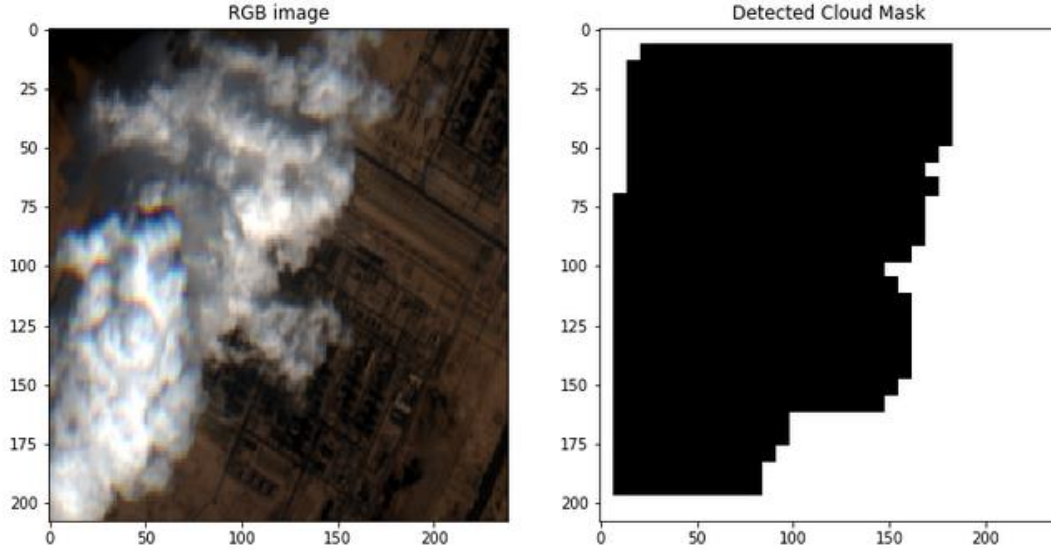
Sources: authors, Kayrros SAS



¹⁰ There is a trade-off as a low threshold entails higher-quality observations (with less distortions by clouds) but deletes more observations. We set a low threshold of 0.07 that empirically maximises the correlation between the satellite-based activity index and ground observations. Correlation depending on the threshold is empirically found to follow a U-shape curve, indicating the presence of the aforementioned trade-off.

Figure 5. Detection of cloud coverage based on RGB images

Sources: authors, Kayrros SAS



2. Interpolating missing observations

A key step consists in interpolating data since a large portion of daily observations can be missing due to a mean revisit time of 3.8 days and to the removal of observations with high cloudiness. Since the data are not missing at random, interpolation is necessary to avoid composition effects when aggregating. Interpolation is based on past observations, seasonal factors, and activity in other plants of the area. The choice of these variables follows industry insights and empirical tests: (i) kilns tend to remain in the same state (“on” or “off”) during long periods since a change of state is expensive, notably for heating the kiln, this justifies the importance of past observations; (ii) shutdowns for maintenance are generally planned around the same date every year, and cement production generally follows the seasonality in construction, hence justifying the inclusion of a seasonal dummy; (iii) finally, activity tends to correlate across all plants, following the overall production cycle in the construction sector.

More formally, we note X_t^i the satellite-based activity index for plant i at day t . We suppose that we have observations only for days $\{\tau_1, \tau_2, \dots, \tau_n\}$. Interpolation for day t follows equation (4) where $X_{\tau_k}^i$ and $X_{\tau_{k-1}}^i$ are the last two available observations for plant i (meaning $\tau_{k+1} > t > \tau_k$), $\underline{X_t^{j \neq i}}$ is the average of the activity indices for other cement plants in the same country at day t , and δ_{month} is a monthly dummy. We allow X_t^i to take values between 0 and 1 instead of only 0 or 1, since this is the activity index for a plant and therefore can be a decimal if only a fraction of the kilns of the plant are active.

$$(4) \quad X_t^i = f \left(X_{\tau_k}^i, X_{\tau_{k-1}}^i, \underline{X_t^{j \neq i}}, \delta_{month} \right)$$

Exploring a range of algorithms for interpolation, we find that the best-performing method relies on a gradient boosting.¹¹ We first test a forward-filling where $X_t^i = X_{t_k}^i$, a naïve simplification in which the activity of a kiln is supposed to be carried on the following days until a change of state is detected. We test also more sophisticated process for equation (4), using a range of options for algorithm f : OLS regression, elastic net (Zou and Hastie, 2005), random forest (Breiman, 2001) and gradient boosting (Friedman, 2001).¹² We perform a 10-fold cross-validation on our full sample: accuracy on “test” data (out-of-sample) is reported in **Table 1** where RMSEs are reported relative to the naïve forward filling. Non-linear techniques – random forest and gradient boosting – yield more accurate estimates with a gain close to 40% compared to forward filling. In the rest of the paper, data are reported after interpolation using gradient boosting.¹³

Table 1. Accuracy relative to naïve forward filling

	<i>OLS</i>	<i>Elastic net</i>	<i>Random forest</i>	<i>Gradient boosting</i>
Relative RMSE	-29.8%	-29.4%	-32.0%	-37.3%

Once the interpolation has been performed for every plant, we aggregate the plant-level time series at country level – in order to match the granularity of the series for cement production. The aggregation is done by weighting each plant by its production capacity, based on industry data. This results in a daily activity index for each country, akin to **Figure 6**.

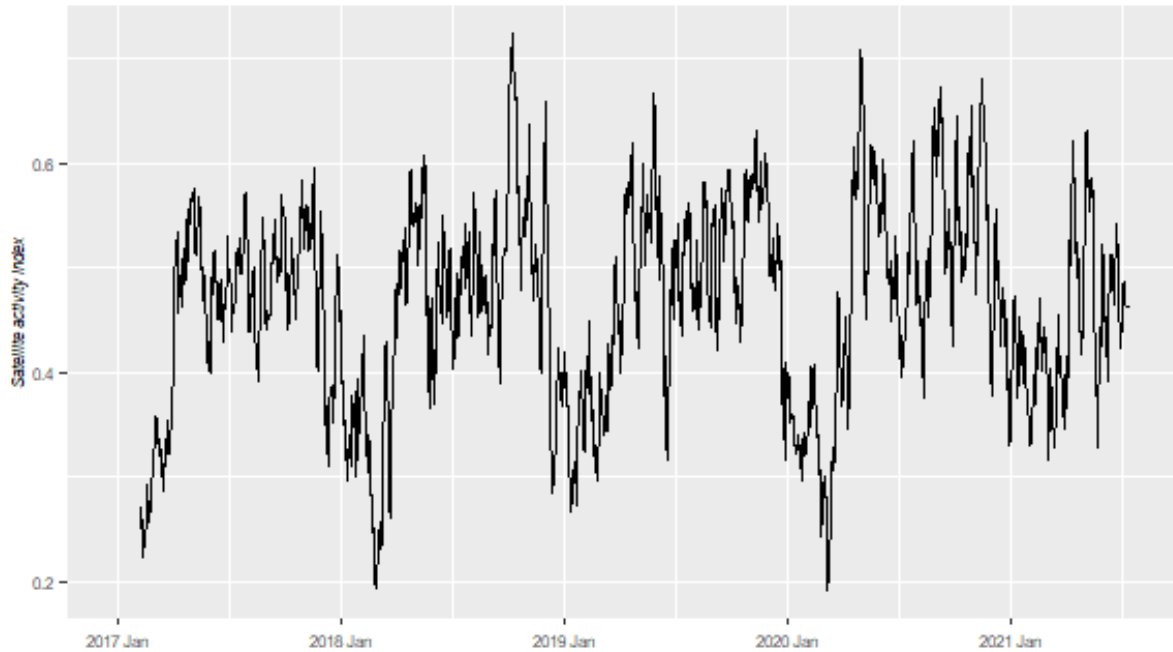
¹¹ We also tested variations of equation (4), for example when using only the last observation or the last three ones (instead of the last two), removing the monthly dummy and the average of other plants in the country, adding a variable to account for the number of days separating current day t from the date of the last observed data point k , or including the cloud coverage. Specification (4) is found empirically to be the best-performing model.

¹² More specifically on the latter, we use the XGBoost method developed by Chen and Guestrin (2016) which has the advantages of high flexibility, faster than other gradient boosting algorithms (notably by resorting to parallel processing) as well as a tendency to yield more accurate forecasts.

¹³ More specifically, we apply equation (4) and gradient boosting where possible, on 70% of the total missing observations. When not possible, our second-best is to apply equation (4) without the average of activity in the other plants of the country – this accounts for 25% of missing observations (e.g. for countries with a small number of plants covered, the average of activity of the other plants in the country is not available for a number of observations). When still not possible – in the beginning of the sample where the second last observation is not available, we apply equation (4) without it (1%). And if the variable on the average of activity in other plants of the country is also not available, we apply equation (4) with only the seasonal dummy and last observation (1%). The remaining 3% is the very beginning of the sample where no “last observation” is available: no interpolation is conducted on these. The first two months are then excluded from the sample to account for it. Before interpolating, we also eliminate from the sample the plants for which the number of observations is too low – but this amounts to only two plants.

Figure 6. Activity index for China (7-day moving average)

Source: authors, Kayrros SAS



Section 4: Nowcasting economic activity

Once we have time series for satellite-based activity index, we assess its predictive power for nowcasting cement production and activity in the construction sector.

1. Comparison to usual benchmark models

We first construct a linear model using the satellite-based activity index to nowcast economic activity. Equation 5 lays out formally our baseline model where the volume of cement production y_t^i in country i at time t is forecasted using our satellite-based index s_t , a constant, and an AR term. To match frequencies between the *monthly* cement production and our *daily* satellite-based activity index s_t , we aggregate the latter by summing daily observations over the month t as in equation 5 where T is the number of days in month t .¹⁴ The second sum accounts for the fact that the country-level index is the weighted average of series s_t^j for individual plant j , with ω^j the weight of plant j .¹⁵ Finally, the model includes an AR term of order 2 (y_{t-2}^i). This is due to the fact that publication delays for cement production are more

¹⁴ In order to account for potential delays in official production declaration, we conducted experiments using various 30-day rolling windows for monthly aggregation by moving the window back in time. Although this approach resulted in a slight improvement in our results, we maintained a calendar-based data aggregation for clarity and to avoid a risk of overfitting.

¹⁵ The weight of each plant is its production capacity scaled by the total production capacity of the country. Production capacity is obtained from industry sources.

than two months in most countries, so in real-time the last available AR term when nowcasting at month t is at most $t - 2$.¹⁶

$$(5) \quad y_t^i = \beta_0^i + \beta_1^i \cdot y_{t-2}^i + \beta_2^i \sum_{\tau \in t} \frac{1}{T} \cdot \left[\sum_{j \in i} \omega^j \cdot s_\tau^j \right] + \varepsilon_t^i$$

We then compare this linear model against common benchmarks – an auto-regressive (AR) model and a random walk (RW) – by conducting a recursive real-time nowcasting exercise that mimics the information that would have been available to a forecaster in real time. To do so, we estimate the model up to month $t - 1$ (*in-sample*) and then nowcast cement production at month t (*out-of-sample*). Then the model is estimated (*in-sample*) up to t and a forecast (*out-of-sample*) is produced for month $t + 1$, and so on. We add one month at each step, following an expanding window strategy. The estimation starts in January 2017, the first out-of-sample is produced for June 2019, and the last one for June 2021. Given publication delays of cement production mentioned above, AR and RW models are of order 2 – as in equation 5.¹⁷ While simplistic benchmarks, AR and RW models are however among the few possibilities to nowcast cement production and construction given the lack of early indicators for this sector.

The linear model with satellite-based activity index is found to outperform these benchmarks, with accuracy gains up to 45% compared to the RW and 25% against the AR. **Table 2** reports the out-of-sample RMSE for the linear model, relative to RW and AR models: negative values indicate outperformance of the linear model. Compared with the AR benchmark, the only difference in our linear model is the inclusion of the satellite-based index, so any accuracy gains can be interpreted as coming from these new data. On average, our linear model outperforms the RW by around 30% and the AR by around 10%. To explore cross-country heterogeneity in relative performances, **Table 2** reports the number of plants covered and the coverage ratio (share of cement plants covered in each country).¹⁸ The coverage ratio does not appear to have a clear correlation with relative performance: for instance, China with a 17% coverage ratio achieves significantly better results than Germany or Brazil with coverage ratios of 65-75%. The number of plants covered seems more clearly correlated with better relative performance for countries with more plants covered (e.g. China, Euro Area, USA).¹⁹

¹⁶ We therefore use AR(2) instead of a country-specific AR term depending on publication delays in each country, for reasons of clarity and cross-country comparability. But it should therefore be noted that for some countries with long publication delays, the AR(2) is a harder benchmark than what would have been for a true real-time forecaster.

¹⁷ In AR, cement production y_t at date t is assumed to depend linearly on a constant 0 and on the production y_{t-2} at date $t-2$. In the latter, y_t is supposed to be equal to y_{t-2} , meaning the RW(2) assumes a constant growth rate.

¹⁸ It should be noted that we track rotary kilns – which still represent 90% of the European production according to CEMBUREAU – and not older technologies (wet kilns for example). This puts an upper bound on possible coverage in our approach.

¹⁹ **Table A1.2** in **Annex 1** also reports results for countries with less than 5 plants covered: while heterogeneous, results are on average not as good as for the countries reported in **Table 2**. A reason for the better results for countries with more plants covered – rather than a higher coverage ratio – might come from the fact that such high-frequency data is noisy, in particular considering the revisit time of 3.8 days (meaning that we have raw observations only every 3.8 days) and the further deletion of observations if biased by cloudiness. With such noisy data, averaging over a high number of plants allows to reduce the idiosyncratic noise inherent to each plant, and *in fine*

We test the significance of differences in predictive accuracy across models through Diebold and Mariano (1995) tests. The OLS model is found to significantly outperform benchmarks in a majority of cases.²⁰ Finally, to counter the risk of overfitting potentially induced by our limited sample (with observations since 2017), we perform a similar analysis with panel regression, which significantly increases the sample size of the regression. Results are reported in **Table A1.3** in **Annex 1** and point to similar findings that the adding the satellite index to the model improves accuracy.²¹

Table 2. Relative RMSE (out-of-sample)

	<i>OLS vs. RW</i>	<i>OLS vs. AR</i>	<i>Plants covered</i>	<i>Coverage ratio</i>
China	-29.7% ***	-15.9% **	143	17%
Euro Area	-45.9% **	-24.3% **	97	74%
<i>Spain</i>	-34.5% *	-13.6% *	25	70%
<i>Germany</i>	-35.5% **	4.7%	25	75%
<i>France</i>	-35.1% **	-13.2% *	24	89%
<i>Italy</i>	-32.5% **	-9.9% *	23	66%
United States	-36.6% **	-13.1% **	69	78%
Brazil	-9.4%	-3.2%	39	65%
Russia	-30.1% **	-14.3% *	35	52%
Mexico	-26.1% **	-16.7% **	27	71%
United Kingdom	-31.1% **	-10.3% *	6	55%
Average	-31.5%	-10.3%	11	65%

*Notes: Period for out-of-sample is June 2019 to June 2021. Results are presented relative to AR and RW models: a negative value indicates an outperformance of the OLS model. Coverage ratio is the share of cement plants covered by Kayrros SAS. ***, **, and * indicate that the outperformance in predictive accuracy of the OLS model with satellite-based data is significant at respectively the 1%, 5%, and 10% levels, based on a one-sided Diebold-Mariano test. Test results are not available for the average.*

2. Comparison to alternative indicators

We then compare the performances of our model with the satellite-based index to models with alternative indicators for the construction sector. It is first key to note the general lack of valid and transparent indicators for construction, an issue raised by Ruddock and Lopes (2006) as well as Hahn and Skudelny (2008), and even more pregnant when it comes to high-frequency indicators. In that respect, our satellite-based index represents a contribution to the literature.

could provide a more reliable indicator for economic activity. The high concentration in the cement industry, with few players having large market shares, could also reduce the predictive power of our indicators in case of oligopoly.

²⁰ The DM test includes the Harvey et al. (1997) corrected variance for small-sample bias.

²¹ In addition, the panel model including the satellite index outperforms the AR model in terms of mean absolute error, AIC, and BIC criteria.

Nonetheless, we compare our model to several other early indicators: (i) Purchasing Managers Index (PMI) which are widely used in the literature to forecast broader industrial production (Bruno and Lupi, 2003; Tsuchiya, 2014; Akdag et al., 2020) and is considered an early indicator given its timely publication (d’Agostino and Schnatz, 2012; Meunier and Jarret, 2022), (ii) Google Trends which are employed in nowcasting following the seminal work of Choi and Varian (2009), for example in McLaren and Shanbhogue (2011) and most notably by Coble and Pincheira (2021) to track activity in construction, and (iii) building permits, an indicator more specific to the construction sector and shown to accurately predict activity for example by Strauss (2013).²²

Table 3. Relative RMSE (out-of-sample)

	<i>Satellite vs. PMI</i>	<i>Satellite vs. Google Trends</i>	<i>Satellite vs. building permits</i>
China	-14.5% **	N.A.	N.A.
Euro Area	-2.5%	-23.2% **	N.A.
<i>Spain</i>	3.2%	-7.7% *	-14.7% **
<i>Germany</i>	-7.9% *	1.9%	-1.2%
<i>France</i>	4.1%	-6.3%	-13.9% *
<i>Italy</i>	-16.1% **	-6.7%	N.A.
United States	-17.9% **	-7.7%	N.A.
Brazil	-7.2%	0.3%	N.A.
Russia	-2.5%	-17.5% **	N.A.
Mexico	-19.3% **	-11.3% *	N.A.
United Kingdom	-3.7%	-12.9% **	N.A.
Average	-7.7%	-9.1%	-9.9%

*Notes: Period for out-of-sample is June 2019 to June 2021. Results are presented relative to benchmark indicator: a negative value indicates over-performance of the OLS model with satellite-based activity index. ***, **, and * indicate that the outperformance in predictive accuracy of the OLS model with satellite-based data is found significant at respectively the 1%, 5%, and 10% levels, based on a one-sided Diebold-Mariano test. Test results are not available for the average.*

Running a real-time out-of-sample nowcasting horserace, the satellite activity index is found to have greater predictive power than the other indicators. **Table 3** shows the relative out-of-sample RMSE of the model with satellite-based index compared with similar models with

²² For PMI indices, we use the PMI manufacturing headline (since there is no index precisely for “cement” or “construction” widely available). For Google Trends, we use the category “Construction & Maintenance” which has the highest degree of correlation with the production of cement. We take the monthly average of weekly Google Trends, even if this indicator may entail some shortcomings since part of searches may be linked to households (especially for do it yourself) with limited impact on cement consumption. A limitation for building permits is however that they might refer to different horizons.

alternative indicators. Results are in relative terms so that a negative value indicates that the model with satellite-based activity outperforms. Models with alternative indicators follow the same specification as in equation 5, only replacing the satellite index by the alternative indicator, so any difference in accuracy can be interpreted as stemming from the use of the satellite index. Using the satellite index leads to gains that can reach around 25% for some countries, and around 10% on average. Differences in predictive accuracy, tested *via* pairwise Diebold-Mariano tests, are found significant in some cases – meaning that the satellite index can significantly improve the nowcasting performances relative to competing indicators.

3. Exploiting the temporal and spatial granularity of the satellite data

After relying on aggregate data, we now explore a more extensive use of the high frequency (daily) and granularity (plant-level) of our satellite index. Our baseline model above relied on a double aggregation at monthly frequency, by averaging daily observations, and country-level, by summing across all plants (see equation 5). As information can be lost when proceeding as such, this section aims at exploiting these temporal and spatial dimensions.

We first test exploiting the time dimension, taking the *daily* satellite index instead of its *monthly* average. We resort to a Mixed Data Sampling (MIDAS) framework (Ghysels et al., 2004) which accounts for the frequency mismatch between daily satellite-based index and monthly data for cement production. The difference with our previous model and the MIDAS is that in the former, each daily observation is given the same coefficient ($\frac{\beta_2^i}{T}$, see equation 5); by contrast, coefficients for daily observations can vary in a MIDAS as shown in equation 6.²³

$$(6) \quad y_t^i = \beta_0^i + \beta_1^i \cdot y_{t-2}^i + \sum_{\tau \in t} \beta_2^i(\tau, \theta^i) \left[\sum_{j \in i} \omega^j \cdot s_\tau^j \right] + \varepsilon_t^i$$

$$\text{where } \beta_2^i(\tau, \theta^i) = \sum_{k=0}^2 \tau^k \cdot \theta_k^i$$

We then turn to exploiting the spatial dimension, using the satellite indices for the *individual* cement plant instead of the country-level *aggregated* index. Doing so increases the number of explanatory variables, so we move away from OLS to techniques suited for high dimensional data sets. We implement a LASSO (Tibshirani, 1996) that estimates a sparse model allocating different coefficients for each plant-level index following equation 7 where coefficients $\beta_2(j)$

²³ The coefficients β_2^i are estimated directly by the MIDAS model. In a MIDAS, the weights generally vary according to a given function in order to discipline individual weights and retain parsimony. We take an “Almon” weighting function (polynomial) of degree $p=3$. While other weighting functions exist (e.g. exponential Almon, step, beta), the “Almon” has the double advantage of flexibility and parsimony as the number of parameters to estimate equals the degree of the “Almon” (3 in our case). This last criterion is key given our limited timespan.

are plant-specific and estimated using the L1 norm penalty of the LASSO.²⁴ It should be noted that the time dimension is not relaxed, and the model still uses monthly averages.

$$(7) \quad y_t^i = \beta_0^i + \beta_1^i \cdot y_{t-2}^i + \sum_{j \in i} \beta_2^i(j) \left[\frac{1}{T} \cdot \sum_{\tau \in t} s_\tau^j \right] + \varepsilon_t^i$$

We finally turn to exploiting both time and spatial dimension, using now the *daily* satellite indices for *individual* cement plants. We use the LASSO-MIDAS of Babii et al. (2021) that combines our two previous set-ups, namely the LASSO for spatial dimension and the MIDAS for temporal dimension. In a LASSO-MIDAS, coefficients are set individually for each daily value of each cement plant following equation 8. Otherwise said, coefficients $\beta_2^{i,j}(\tau)$ are not only plant-specific but also differ depending on the day. The β_2 coefficients follow Legendre polynomials, in line with Babii et al. (2021).

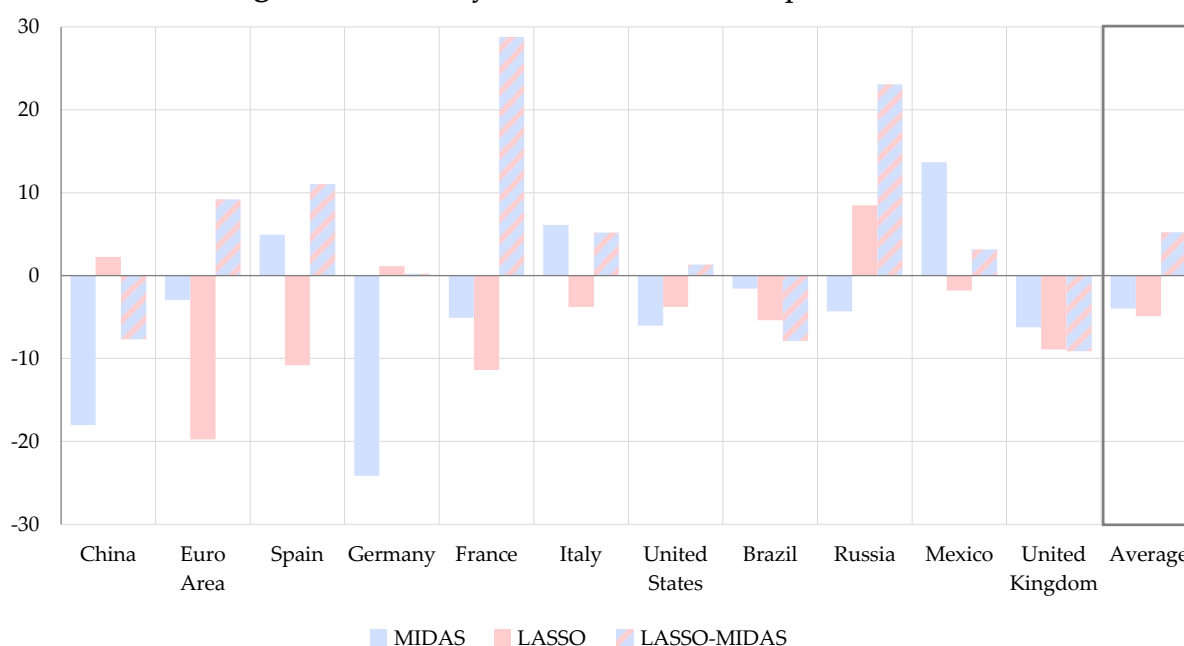
$$(8) \quad y_t^i = \beta_0^i + \beta_1^i \cdot y_{t-2}^i + \sum_{\tau \in t} \sum_{j \in i} \beta_2^{i,j}(\tau) \cdot s_\tau^j + \varepsilon_t^i$$

Empirically, the gains in accuracy are however very limited when relaxing temporal and/or spatial dimensions, even though some improvement can be reached. **Figure 7** presents the accuracy of the alternative regression techniques (MIDAS, LASSO, LASSO-MIDAS) to the OLS set-up used in **sections 4.1** and **4.2**. The comparison is conducted out-of-sample over June 2019 to June 2021. As shown by equations 5 to 8, the set-ups differ only in terms of relaxing temporal and/or spatial dimensions: the underlying data remain identical, as well as the transformations and lags of the dependent variable (y_t^i). Any difference can then be interpreted as the effect of exploiting (or not) temporal and/or spatial dimension. **Figure 7** is represented in terms of the relative accuracy to the model using the satellite index aggregated at monthly frequency and country-level. A negative value means that the model on *aggregated* data outperforms the alternative techniques on *disaggregated* data. In general, performances are not improved by using disaggregated data although there are some accuracy gains in a few countries (e.g. Russia and Spain). The LASSO-MIDAS is however performing somehow better than the OLS on aggregated data, notably for some countries (e.g. France and Russia). On average (rightmost panel), performances with *disaggregated* data are however generally not significantly different from the OLS on *aggregated* data.

²⁴ LASSO is a class of penalized regressions which, instead of minimizing the sum of squared residuals $\sum (y_i - \beta_i \cdot x_i)^2$ as in an OLS, will elect coefficients that minimize the sum of squared residuals with a penalty – which is the L1 norm of coefficients as in the equation below. The sparsity penalty (λ) is chosen such that error is within one standard error of the minimum, using a 10-fold validation on in-sample data.

$$\sum_i (y_i - \beta_i \cdot x_i)^2 + \lambda \cdot \|\beta\|_1$$

Figure 7. Accuracy of alternative techniques relative to OLS



Notes: The y-axis represents the accuracy compared to the OLS set-up based on the satellite index aggregated at monthly frequency and country level. A negative value means the OLS on **aggregated** data outperforms the alternative technique on **disaggregated** data. MIDAS uses daily data; LASSO uses plant-level data; LASSO-MIDAS uses daily plant-level data. Accuracy is measured by the out-of-sample RMSE over June 2019 to June 2021.

4. Exploring non-linearities with neural networks

While models up until now have remained linear, we now turn to exploring non-linearities between cement production and our satellite index. This is motivated by the fact that, with *individual* plant-level indices, there could be non-linearities from interactions between the different series. Non-linear models in this section are therefore based on the *disaggregated* plant-level data. In addition, non-linearities can also arise from the fact that the target variable appears rather volatile (Table A1.4 in Annex 1).

We use neural networks which, compared with other non-linear methods, have the double advantage of: (i) allowing for a large number of non-linearities, and (ii) being generally found of high predictive power (see Makridakis et al., 2020). We employ a multi-layer perceptron with a limited number of hidden layers, to avoid overfitting given the small size of the data. We set a limited number of neurons with each neuron using a hyperbolic tangent (*tanh*) activation function. This choice is guided by the fact that the variations of the independent variables are relatively limited and centred around 0; the high derivative of the hyperbolic tangent function at 0 allows these small values to be amplified to match the high variations of the dependent variable (see Table A1.4 in Annex 1). The weights are optimised using the stochastic gradient descent of Adam optimizer (Kingma and Ma, 2017) as is standard in the literature. Given the limited timespan, we set the batch size (number of observations the algorithm uses before adjusting parameters) at a minimal value. To prevent overfitting, we keep the number of epochs (number of times the algorithm runs through the in-sample set)

moderate and we add dropout layers (intermediate layer in the neural network in which a percentage of neurons is randomly muted) after each hidden layer.²⁵ Finally, since neural networks are sensitive to the initial parameters (Woloszko, 2020), we average the predictions of an ensemble of five neural networks initialised with different random initial parameters – in order to limit the effect of randomness.

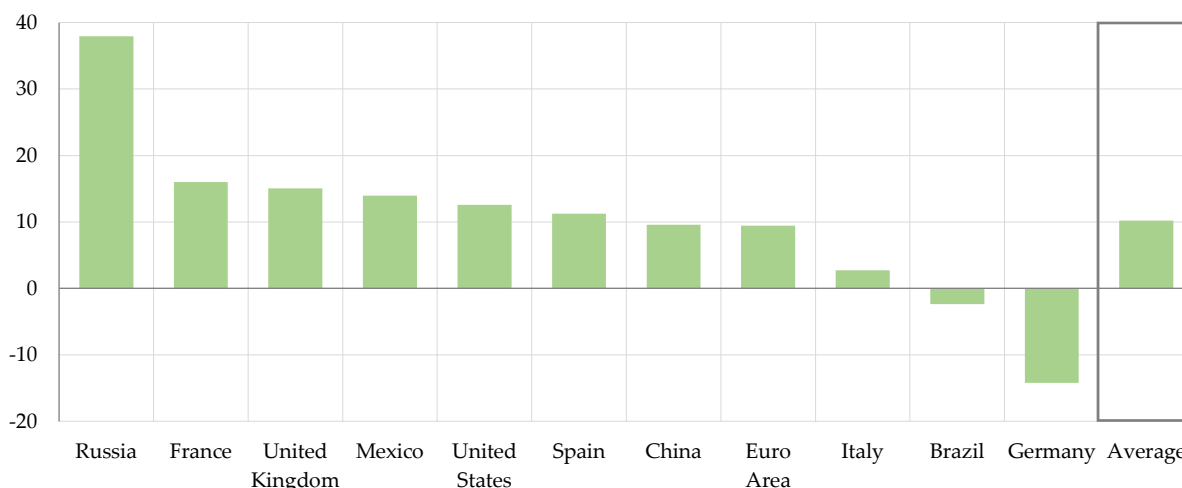
Using neural networks yields improvements in accuracy, with gains up to 40% compared with the linear model, although gains are heterogenous across countries. **Figure 8** presents the accuracy of the neural networks compared with the OLS set-up of **sections 4.1** and **4.2**. The comparison is conducted out-of-sample over June 2019 to June 2021. Results are represented in terms of relative accuracy to the linear set-up, so that a positive value indicates an outperformance of the neural network – with the value in the y-axis showing by how much percent accuracy changes. Overall, forecasting performances are improved by neural networks with accuracy gains up to almost 40% for Russia. Performances are however heterogenous across countries, with little to no improvement in some (e.g. Italy, Brazil, Germany).²⁶ But on average, using a non-linear framework improves performances by around 10%, which seems to confirm the intuition that the relationship between cement production and our satellite index is non-linear. It also confirms the potential of neural network in nowcasting, in line with Woloszko (2020) and Hopp (2021). Finally, it also supports conclusions of Olson et al. (2018) that neural networks are able to perform well even on small, noisy data sets.²⁷

²⁵ We set hyperparameters by simple trial-and-error process as recommended in Woloszko (2020) in order to avoid the “overfitting on the validation set” that can arise when using grid search. For the number of epochs, a trade-off appears: a high number of epochs is necessary to ensure proper learning on the one side (given the limited size of the data, the stochastic gradient descent algorithm would need to run multiple times through the data to adjust all model parameters) but on the other side can lead to overfitting. Considering this, we set a limited number of epochs (20). On top of number of layers (3), number of neurons (521 on first layer, then decreasing by a factor 2 in each layer), number of epochs (20), and batch size (1), we also tested for other hyper-parameters whose importance was however found to be less crucial: other activation functions than the *tanh*, different weight initializers (we use *random uniform*), presence of batch normalization layers, and addition of a penalty for kernel regularizers (with L2 norm). Finally, averaging over an ensemble of neural networks, as is done on this paper, also reduces the concerns of overfitting.

²⁶ Heterogeneity might come from the trial-and-error selection of hyper-parameters which implies that they can be less optimal for some zones. Another approach would have been to run the selection of hyper-parameters for each country individually, but it comes at the risk of overfitting.

²⁷ We also tried to exploit both spatial and temporal dimensions in a neural network, using daily data disaggregated by plant as input. Results are however limited. A first explanatory factor can be the higher number of parameters in this case, with up to 4,000 observations as inputs and therefore millions of parameters to estimate for the model. Due to the limited sample, none of the tested neural networks outperformed the linear model – when using a global parametrization.

Figure 8. Accuracy of neural network relative to OLS



Notes: The y-axis represents the accuracy compared to the OLS set-up based on the satellite index aggregated at monthly frequency and country level. A positive value means the neural network outperforms the OLS. The neural network uses plant-level data. Predictions of neural network are the average of an ensemble of 10 models initialized with different random weights. Accuracy is measured by the out-of-sample RMSE over June 2019 to June 2021.

5. Nowcasting regional activity

In the previous sections, we mostly emphasised the granularity of our data along the time dimension, allowing us to develop a powerful and accurate real-time indicator. However, the spatial dimension is also worthy of interest. Since cement is not usually trucked nor shipped over long distances, cement plants can be found near most major cities and industrial areas. This can allow to develop indicators at the sub-national level to monitor regional activity. In this vein, we perform a similar exercise over regions in the United States – the only country for which regional cement production data are available. In order to have a sufficient sample number of plants, we divide the US into 9 regions.²⁸ Results are reported in **Table 4**: although they differ among regions, the OLS model outperforms strongly the AR(2) model in some regions, or does not differ significantly from it.²⁹ This suggests the validity of the approach to also track economic activity at the regional level.

Table 4. Relative RMSE (out-of-sample) for US regions

	Satellite vs. AR(2)	Number of plants
New-York	-14%	9
Washington	1%	11
California	-9.1%	11
Illinois	2.5%	8

²⁸ States in **Table 4** are the main states of each larger US region.

²⁹ Note that two of the coldest regions of the United States – North-west and central – obtain the worst results. This may arise from an important seasonality in the construction industry caused by extreme weather conditions during winter.

Michigan	-2.1%	2
Texas	-1.7%	7
Florida	0.6%	11
Iowa	-0.2%	4
Missouri	-1.2%	4
Average	-2.3%	-

Notes: Period for out-of-sample is June 2019 to June 2021. Results are presented relative to an AR(2): a negative value indicates outperformance of the OLS model.

6. Nowcasting activity in the construction sector

Having shown that the satellite-based activity index has a significant predictive power for cement production, we now question whether our satellite index retains such interest for broader economic conditions, notably activity in construction. We perform a similar exercise as in **sections 4.1** and **4.2** but using the volume of construction as a dependent variable. We compare an OLS model with satellite to RW and AR benchmarks, as well as similar models based on building permits, PMI, and Google Trends.

Results suggest that the model with satellite-based index can outperform benchmarks, simple AR and RW as well as models based on alternative indicators, also when nowcasting activity in the construction sector. **Table 5** summarises the results of the horserace, showing the RMSE of the linear model with the satellite-based index relative to others, so that a negative value indicates an outperformance of the model with the satellite index. On average, using satellite-based data improves accuracy of the nowcasts by 5% to 15% compared to other indicators such as Google Trends, PMIs, and building permits. Improvements in nowcast accuracy are generally found significant *vs.* RW and AR, as well as *vis-à-vis* models based on alternative indicators in a number of cases. Overall, these results suggest the ability of the satellite-based data to not only accurately nowcast developments in the cement production but also more broadly in the construction industry.

Table 5. Relative RMSE (out-of-sample)

	<i>Satellite vs. RW</i>	<i>Satellite vs. AR</i>	<i>Satellite vs. PMIs</i>	<i>Satellite vs. GT</i>	<i>Satellite vs. permits</i>
China	-6.3%	-18.6% *	-14.5%	N.A.	N.A.
Euro Area	-39.1% ***	-22.4% *	-1.3%	-20.6% *	N.A.
<i>Spain</i>	-29.8% **	-21.7% **	-11.7%	-19.7% **	-7.7%
<i>Germany</i>	-28.5% **	10.8%	-0.7%	6.0%	6.5%
<i>France</i>	-35.0% **	-18.8% *	3.6%	-9.4%	-17.4% **
<i>Italy</i>	-35.9% **	-15.1%	1.5%	-12.8%	N.A.
United States	0.0%	-2.3%	-24.8% *	-7.5%	N.A.
Brazil	-16.0% *	-10.6%	-11.7%	-8.6%	N.A.
Russia	N.A.	N.A.	N.A.	N.A.	N.A.
Mexico	N.A.	N.A.	N.A.	N.A.	N.A.
United Kingdom	-14.0% *	-34.4% **	6.9%	-31.3% **	N.A.
Average	-22.7%	-14.8%	-5.9%	-13.0%	-6.2%

Notes: Period for out-of-sample is June 2019 to June 2021. Results are presented relative to AR and RW models: a negative value indicates over-performance of the OLS model. Coverage ratio is the share of cement plants covered by our technology. ***, **, and * indicate that the outperformance in predictive accuracy of the OLS model with satellite-based data is found significant at respectively the 1%, 5%, and 10% levels, based on a one-sided Diebold-Mariano test. Test results are not available for the average.

Section 5: Conclusions

By exploiting satellite images over cement plants, this paper builds a daily index of activity in the cement industry. The choice to focus on cement plants is motivated by three facts: the wide use of cement in construction, the possibility to detect the heat of cement plants with satellites, and the scarcity of early indicators for activity in the construction sector. While satellite images have remained largely untapped in the economic literature so far, this paper provides a blueprint for retrieving images, exploiting the characteristics of infrared emissions, cleaning raw data with AI image recognition (to correct for cloud coverage) and interpolating missing data with a gradient boosting algorithm. Applying this method to more than 500 plants in our sample, this paper provides a daily activity index for 42 countries.

We use these satellite-based data to track in real-time both the production of cement and the activity in the construction sector, using linear models as well as neural networks. Starting with a simple linear framework, where the daily index is averaged over the month, this paper shows that nowcasting cement production with these satellite-based data significantly improves accuracy – not only relative to simple auto-regressive and random walk models, but also when compared with models based on alternative indicators used in the literature

(building permits, PMIs, and Google Trends). Exploiting more deeply the spatial and temporal dimensions, we report similar accuracy when using LASSO, MIDAS, and LASSO-MIDAS that uses the full granularity of the *daily* and *plant-level* satellite indices. We finally turn to neural networks to explore non-linearities in the relation between the satellite index and economic activity. We report some large gains when using such a non-linear framework, in line with the recent literature using neural networks for nowcasting.

Limitations on the timespan and the availability of official statistics however makes it more challenging to test predictive capacities more broadly. In particular, the small sample size is most likely not sufficient to reach optimal accuracy. Therefore, results in this paper can be viewed as a lower bound for attainable accuracy – which would improve over time as more satellite observations become available. Finally, while this paper focuses on cement plants, it provides a methodology to track activity in other heat-emitting sectors such as steel and iron, or extractive industries.³⁰ It may also enable to cover activity in these sectors in emerging and developing countries, including on an infra-yearly frequency, and to follow activity at sub-national level when the number of plants is high enough.

³⁰ While this is possible that future cement production technologies emit less heat and therefore complicates the capture of production through our index, such technologies are still nascent. In France, they are expected to reach at most 3% of total production in 2024 (see for example [this article](#)).

References

- Aaronson, D., Brave, S., and Cole, R. (2016). "Using private sector "big data" as an economic indicator: The case of construction spending", *Chicago Fed Letter*, No 366.
- d'Agostino, A., and Schnatz, B. (2012). "Survey-based nowcasting of US growth: a real-time forecast comparison over more than 40 years", *Working Paper Series*, No 1455, European Central Bank.
- Akdag, S., Deran, A., and Iskenderoglu, O. (2020). "Is PMI a Leading Indicator: Case of Turkey", *Sosyoekonomi Journal*, 28(45).
- Akiba, T., Sano, S., Yanase, T., Ohta, T., and Koyama, M. (2019). "Optuna: A Next-generation Hyperparameter Optimization Framework", arXiv pre-print.
- Alagidede, P., and Odei Mensah, J. (2018). "Construction institutions and economic growth in sub-Saharan Africa", *African Review of Economics and Finance*, 10(1) — June.
- Babii, A., Ghysels, E., and Striaukas, J. (2021). "Machine Learning Time Series Regressions with an Application to Nowcasting", *Journal of Business & Economic Statistics*.
- Berk, N., and Bicen, S. (2018). "Causality between the Construction Sector and GDP Growth in Emerging Countries: The Case of Turkey", *Athens Journal of Mediterranean Studies*, 4(1), pp. 19–36.
- Bergstra, J., Yamins, D., and Cox, D. (2013). "Making a Science of Model Search: Hyperparameter Optimization in Hundreds of Dimensions for Vision Architectures", *Proceedings of the 30th International Conference on Machine Learning*.
- Beyer, R., Franco-Bedoya, S., and Galdo, V. (2021). "Examining the economic impact of COVID-19 in India through daily electricity consumption and night-time light intensity", *World Development*, 140.
- Bon, R. (1992). "The future of international construction: secular patterns of growth and decline", *Habitat International*, 16(3), pp. 119–128.
- Bon, R., and Pietroforte, R. (1990). "Historical comparison of construction sectors in the United States, Japan, Italy and Finland using input-output tables", *Construction Management and Economics*, 8, pp. 233–247.
- Breiman, L. (2001). "Random Forests", *Machine Learning*, 45, pp. 5–32.
- Bricongne, J.-C., Coffinet, J., Delbos, J.-B., Kaiser, V., Kien, J.-N., Kintzler, E., Lestrade, A., Meunier, B., Mouliom, M., and Nicolas, T. (2020). "Tracking the economy during the Covid-19 pandemic: The contribution of high-frequency indicators", *Bulletin de la Banque de France*, 231.

- Bricongne, J.-C., Meunier, B., and Pical, T. (2021). "Can satellite data on air pollution predict industrial production?", *Working papers*, No 847, Banque de France.
- Bricongne J.-C., Meunier B., and Pouget, S. (2023). "Web Scraping Housing Prices in Real-time: the Covid-19 Crisis in the UK", *Journal of Housing Economics*, 59.
- Bruno, G., and Lupi, C. (2003). "Forecasting euro-area industrial production using (mostly) business surveys data", *ISAE Working Papers*, No 33.
- Buckmann, M., and Joseph, A. (2022). "An Interpretable Machine Learning Workflow with An Application to Economic Forecasting", *Bank of England Working Paper*, No. 984.
- Chen, T., and Guestrin, C. (2016). "XGBoost: A Scalable Tree Boosting System", in *Proceedings of the 22nd ACM SIGKDD International Conference on Knowledge Discovery and Data Mining*, pp. 785–794.
- Chen, X., and Nordhaus, D. (2010). "Using luminosity data as a proxy for economic statistics", *Proceedings of the National Academy of Sciences*, 108(21), pp. 8589– 8594.
- Chetty, R., Friedman, J., Hendren, N., Stepner, M., and the Opportunity Insights Team (2020). "How Did COVID-19 and Stabilization Policies Affect Spending and Employment? A New Real-Time Economic Tracker Based on Private Sector Data", *NBER Working Paper*, No 27431.
- Chien, S., Sherwood, R., Tran, D., Cichy, B., Rabideau, G., Castano, R., Davies, A., Mandl, D., Frye, S., Trout, B., d'Agostino, J., Shulman, S., Boyer, D., Hayden, S., Sweet, A., and Christa, S. (2005). "Lessons learned from autonomous sciencecraft experiment", *Proceedings of the fourth international joint conference on Autonomous agents and multiagent systems*, July, pp. 11–18.
- Chodorow-Reich, G., Gopinath, G., Mishra, P., and Narayanan, A. (2020). "Cash and the Economy: Evidence from India's Demonetization", *The Quarterly Journal of Economics*, 135(1), pp. 57–103.
- Choi, H., and Varian, H. (2009). "Predicting the Present with Google Trends", *SSRN Electronic Journal*, <http://dx.doi.org/10.2139/ssrn.1659302>.
- Civelli, A., Horowitz, A., and Teixeira, A. (2018). "Foreign aid and growth: A Sp P-VAR analysis using satellite sub-national data for Uganda", *Journal of Development Economics*, 134, pp. 50–67.
- Coble, D., and Pincheira, P. (2021). "Forecasting building permits with Google Trends", *Empirical Economics*, 61, pp. 3315–3345.
- Combinido, J., Mendoza, J., and Aborot, J. (2018). "A Convolutional Neural Network Approach for Estimating Tropical Cyclone Intensity Using Satellite-based Infrared Images", *24th International Conference on Pattern Recognition proceedings*, pp. 1474–1480.

- Deakshinamurthy, A. (2017). "Demand forecasting for cement in India 2030", *International Journal of Marketing & Financial Management*, 5(8), pp. 9–13.
- De Long, J., and Summers, L. (1991). "Equipment investment and economic growth", *The Quarterly Journal of Economics*, 106, pp. 445–502.
- Diebold F. and Mariano R. (1995). "Comparing predictive accuracy", *Journal of Business and Economic Statistics*, 13, pp. 253–263.
- Donaldson, D., and Storeygard, A. (2016). "The View from Above: Applications of Satellite Data in Economics", *Journal of Economic Perspectives*, 30(4), pp. 171–198.
- Ebener, S., Murray, C., Tandon, A., and Elvidge, C. (2005). "From wealth to health: modelling the distribution of income per capita at the subnational level using night-time light imagery", *International Journal of Health Geographics*, 4(5).
- Friedman, J. (2001). "Greedy function approximation: a gradient boosting machine", *Annals of Statistics*, 29(5), pp. 1189–1232.
- Gagg, C. (2014). "Cement and concrete as an engineering material: An historic appraisal and case study analysis", *Engineering Failure Analysis*, 40, pp. 114–140.
- Ghosh, T., Anderson, S., Powell, R., Sutton, P., and Elvidge, C. (2009). "Estimation of Mexico's Informal Economy and Remittances Using Night-time Imagery", *Remote Sensing*, 1, pp. 418–444.
- Ghysels, E., Santa-Clara, P., and Valkanov, R. (2004). "The MIDAS Touch: Mixed Data Sampling Regression Models", *CIRANO Working Papers*, No 2004-20.
- Gomez, A. L., and del Carmen Sanchez, M. (2017). "Indicators to monitor and follow construction investment", *Occasional Papers*, No 1705, Banco de España.
- Hahn, E., and Skudelny, F. (2008). "Early estimates of euro area real GDP growth: a bottom up approach from the production side", *Working Paper Series*, No 975, European Central Bank.
- Harvey D., Leybourne S. and Newbold P. (1997). "Testing the equality of prediction mean squared errors", *International Journal of Forecasting*, 13(2), pp. 281–291.
- Henderson, J., Storeygard, A., and Weil, D. (2012). "Measuring Economic Growth from Outer Space", *American Economic Review*, 102(2), pp. 994–1028.
- Hong, L. (2014). "The Dynamic Relationship between Real Estate Investment and Economic Growth: Evidence from Prefecture City Panel Data in China", *IERI Procedia*, 7, pp. 2–7.
- Hopp, D. (2021). "Economic Nowcasting with Long Short-Term Memory Artificial Neural Networks (LSTM)", *arXiv pre-print*.

- Jardet, C., and Meunier, B. (2022). "Nowcasting World GDP Growth with High-Frequency Data", *Journal of Forecasting*, 41(6), pp. 1181–1200.
- Jiang, Q. (2013). "Analysis on the Relationship between GDP and Construction Based on the Data of UK and China", *Proceedings of the 2013 Conference on Education Technology and Management Science*, Atlantis Press, pp. 1378–1381.
- Joseph, A. (2019). "Opening the machine learning black box", *Bank Underground*, Bank of England, 24 May.
- Kalvova, J., Halenka, T., Bezpalcova, K., and Nemesova, I. (2003). "Koppen climate types in observed and simulated climates", *Studia Geophysica et Geodaetica*, pp. 185–202.
- Kingma, D., and Ba, J. (2017). "Adam: A Method for Stochastic Optimization", *arXiv pre-print*.
- Kumo, W. (2012). "Infrastructure Investment and Economic Growth in South Africa: A Granger Causality Analysis", *Working Paper Series*, No 160, African Development Bank.
- Lean, C. (2001). "Empirical tests to discern linkages between construction and other economic sectors in Singapore", *Construction Management, and Economics Journal*, 19(4), pp. 355–363.
- Li, N., Ma, D., and Chen, W. (2015). "Projection of cement demand and analysis of the impacts of carbon tax on cement industry in China", *Energy Procedia*, 75, pp. 1766–1771.
- Makridakis, S., Spiliotis, E., and Assimakopoulos, V. (2020). "The M4 Competition: 100,000 time series and 61 forecasting methods", *International Journal of Forecasting*, 36(1), pp. 54–74.
- Massimetti, F., Coppola, D., Laiolo, M., Valade, S., Cigolini, C., and Ripepe, M. (2020). "Volcanic Hot-Spot Detection Using SENTINEL-2: A Comparison with MODIS-MIROVA Thermal Data Series", *Remote Sensing*, 12(5), 820.
- McLaren, N., and Shanbhogue, R. (2011). "Using internet search data as economic indicators", *Bank of England Quarterly Bulletin*, Q2.
- Munro, J., Medina, I., Walker, K., Moussalli, A., Kearney, M., Dyer, A., Garcia, J., Rankin, K., and Stuart-Fox, D. (2019). "Climate is a strong predictor of near-infrared reflectance but a poor predictor of colour in butterflies", *Proceedings of the Royal Society B: Biological Sciences*, 286(1898).
- Murphy, S., Roberto de Souza Filho, C., Wright, R., Sabatino, G., and Correa Pabon, R. (2016). "HOTMAP: Global hot target detection at moderate spatial resolution", *Remote Sensing of Environment*, 177, pp. 78–88.
- Olson, M., Wyner, A., and Berk, R. (2018). "Modern Neural Networks Generalize on Small Data Sets", *Neural Information Processing Systems*.

- Pinkovskiy, M., and Sala-i-Martin, X. (2016). "Lights, Camera . . . Income! Illuminating the National Accounts-Household Surveys Debate", *The Quarterly Journal of Economics*, 131(2), pp. 579–631.
- Poggiali, G., Brucato, J. R., Dotto, E., Ieva, S., Barucci, M. A., and Pajola, M. (2021). "Temperature dependent mid-infrared (5–25 μm) reflectance spectroscopy of carbonaceous meteorites and minerals: Implication for remote sensing in Solar System exploration", *Icarus*, 354, 114040.
- Ruddock, L., and Lopes, J. (2006). "The construction sector and economic development: the 'Bon curve'", *Construction Management and Economics*, 24(7), pp. 717–723.
- Scambos, T., Campbell, G., Pope, A., Haran, T., Muto, A., Lazzara, M., Reijmer, C., and van den Broeke, M. (2018). "Ultralow Surface Temperatures in East Antarctica From Satellite Thermal Infrared Mapping: The Coldest Places on Earth", *Geophysical Research Letters*, 45(12), pp. 6124–6133.
- Strassmann, P. (1970). "The construction sector in economic development", *The Scottish Journal of Political Economy*, 17, pp. 390–410.
- Strauss, J. (2013). "Does housing drive state-level job growth? Building permits and consumer expectations forecast a state's economic activity", *Journal of Urban Economics*, 73(1), pp. 77–93.
- Sutton, P., Elvidge, C., and Ghosh, T. (2007). "Estimation of Gross Domestic Product at Sub-National Scales using Night-time Satellite Imagery", *International Journal of Ecological Economics Statistics*, 8(S07), pp. 5–21.
- Tanaka, K., and Keola, S. (2017). "Shedding Light on the Shadow Economy: A Night-time Light Approach", *The Journal of Development Studies*, 53(1), pp. 32–48.
- Tibshirani, R. (1996). "Regression shrinkage and selection via the LASSO", *Journal of the Royal Statistical Society: Series B*, 58(1), pp. 267–288.
- Tsuchiya, Y. (2014). "Purchasing and supply managers provide early clues on the direction of the US economy: An application of a new market-timing test", *International Review of Economics & Finance*, 29, pp. 599–618.
- Uzzaman, I., Rahman, M., Alam, S., and Alam, S. (2016). "Simulation of Cement Manufacturing Process and Demand Forecasting of Cement Industry", *Global Journal of Researches in Engineering*, 16(2).
- Wilinski, D., Kantorowicz, J., and Wierzchon, S. (2016). "Modelling the demand for cement: The case of Poland and Spain", *Journal of Building Chemistry*, 1, pp. 69–83.

Woloszko, N. (2020). "Tracking activity in real time with Google Trends", *Working Papers*, No 1634, OECD Economics Department.

Zou, H., and Hastie, T. (2005). "Regularization and Variable Selection via the Elastic Net", *Journal of the Royal Statistical Society Series B*, 67(2), pp. 301–320.

Annex 1: supplementary tables

Table A1.1. Data sources for cement production (volumes)

<i>Country</i>	<i>Sector</i>	<i>Source</i>
Austria	Other non-metallic mineral products	Eurostat
Belgium	Other non-metallic mineral products	Eurostat
Bosnia and Herzegovina	Manufacturing	Eurostat
Brazil	Cement	IBGE (statistics Brazil)
Bulgaria	Other non-metallic mineral products	Eurostat
Canada	Cement and concrete products	Statistics Canada
China	Cement	National Bureau of Statistics China
Croatia	Manufacturing	Eurostat
Cyprus	Manufacturing	Eurostat
Czechia	Other non-metallic mineral products	Eurostat
Denmark	Other non-metallic mineral products	Eurostat
Estonia	Other non-metallic mineral products	Eurostat
Finland	Other non-metallic mineral products	Eurostat
France	Cement	Eurostat
Germany	Cement	Eurostat
Greece	Cement	Eurostat
Hungary	Other non-metallic mineral products	Eurostat
Italy	Cement	Eurostat
Latvia	Other non-metallic mineral products	Eurostat
Lithuania	Cement, lime, and plaster	Eurostat
Luxembourg	Manufacturing	Eurostat
Mexico	Cement (white cement)	INEGI
Netherlands	Other non-metallic mineral products	Eurostat
North Macedonia	Other non-metallic mineral products	Eurostat
Norway	Other non-metallic mineral products	Eurostat
Poland	Other non-metallic mineral products	Eurostat
Portugal	Other non-metallic mineral products	Eurostat
Romania	Other non-metallic mineral products	Eurostat
Russia	Cement, lime, and plaster	Rosstat
Serbia	Manufacturing	Eurostat
Slovakia	Manufacturing	Eurostat
Slovenia	Manufacturing	Eurostat
Spain	Cement	Eurostat
Sweden	Other non-metallic mineral products	Eurostat
Switzerland	Manufacturing	Eurostat
Ukraine	Clinker	State Statistics Ukraine
United Kingdom	Other non-metallic mineral products	Eurostat
United States	Clinker	USGS

Table A1.2. Relative RMSE (out-of-sample) – countries with less than 5 plants covered

	<i>OLS vs. RW</i>	<i>OLS vs. AR</i>	<i>Plants covered</i>	<i>Coverage ratio</i>
Austria	-10.2%	0.8%	4	45%
Belgium	-20.5%	-0.6%	4	100%
Croatia	-0.3%	3.8%	4	100%
Czechia	-11.6%	2.0%	4	80%
Hungary	-5.2%	1.0%	4	N.A.
Slovakia	-5.1%	-1.1%	4	80%
Bulgaria	-6.7%	0.4%	3	75%
Serbia	-24.8%	-0.2%	3	100%
Sweden	-33.1%	2.1%	3	N.A.
Switzerland	-2.5%	-2.3%	3	50%
Bosnia and Herzegovina	-4.6%	-4.2%	2	100%
Finland	-17.0%	0.7%	2	100%
Cyprus	-18.9%	0.2%	1	100%
Denmark	1.1%	0.1%	1	50%
Estonia	13.1%	3.3%	1	N.A.
Latvia	-30.8%	-6.2%	1	100%
Lithuania	-5.5%	0.2%	1	100%
Luxembourg	-8.2%	0.8%	1	N.A.
Netherlands	-24.7%	0.3%	1	N.A.
North Macedonia	-28.4%	-1.1%	1	100%
Norway	-29.7%	-8.6%	1	50%
Slovenia	-14.5%	-6.1%	1	100%
Average	-13.1%	-0.6%	2.7	84%

Notes: Period for out-of-sample is June 2019 to June 2021. Results are presented relative to AR and RW models: a negative value indicates over-performance of the OLS model. Coverage ratio is the share of cement plants covered by our technology.

Table A1.3. Relative RMSE (out-of-sample) – Panel Model

	<i>Satellite vs AR(2)</i>	<i>Number of plants</i>
Italy	-5.1%	23
France	-7%	23
Germany	-0.9%	24
Greece	-4.2%	6
Spain	-15.6%	25
Russia	-14.8%	35
Romania	-16.2%	7
Poland	-21.2%	9
Mexico	-16.7%	27
China	-9.7%	143
Brazil	-16.5%	37
United States	-8.7%	67
Average	-11.4%	-

Notes: Period for out-of-sample is June 2019 to June 2021. Results relative to AR models: a negative value indicates an outperformance of the model with satellite index

Table A1.4. Descriptive statistics

	Cement production (y-o-y growth, %)				Satellite-based index (y-o-y, difference)			
	25 th	Median	75 th	IQR	25 th	Median	75 th	IQR
China	-8.5	-0.8	7.2	15.6	-0.02	0.01	0.04	0.06
Spain	-6.5	4.3	9.8	16.3	-0.08	0.00	0.06	0.14
Germany	-9.6	-1.7	11.4	21.0	-0.05	0.00	0.04	0.08
France	-14.7	-0.2	15.1	29.9	-0.07	0.02	0.06	0.13
Italy	-15.9	-2.7	16.5	32.4	-0.02	-0.01	0.03	0.05
United States	-5.8	-0.1	7.0	12.8	-0.02	0.01	0.04	0.06
Brazil	-2.3	4.3	14.7	17.0	-0.04	0.02	0.10	0.14
Russia	-14.5	-2.0	12.9	27.4	-0.05	-0.02	0.03	0.08
Mexico	-5.6	5.2	19.8	25.5	-0.06	-0.02	0.08	0.14
United Kingdom	-13.0	-7.8	-1.9	11.1	-0.07	0.00	0.10	0.17
Average	-9.6	-0.1	11.3	20.9	-0.05	0.00	0.06	0.11

Note: Statistics over full sample (Jan. 2017 to June 2021). Results for cement production are in year-on-year percentage change. Results for satellite-based index are in year-on-year difference which, by construction of the satellite index, is bounded between -1 and +1. IQR = inter-quartile range, computed as the difference between the 25th and 75th percentiles. It measures the dispersion of series, while being less distorted by outliers (such as the Covid-19 crisis) than the standard deviation.